J|A|C|S
ARTICLES
Published on Web 06/07/2005

Single-Crystal Studies of Peptide Prolyl and Glycyl ^{15}N Shielding Tensors

Kevin W. Waddell, Eduard Y. Chekmenev,† and Richard J. Wittebort*

Contribution from the Department of Chemistry, 2320 South Brook Street, University of Louisville, Louisville, Kentucky 40292

Received September 23, 2004; E-mail: rjwitt01@louisville.edu

Abstract: ^{15}N shielding tensors were determined for the central peptide groups in GGV, AGG, and APG by single-crystal NMR. We find that the angle between the downfield component (δ_{11}) and the N−H or the N−C$^{\delta}$ (pro) bonds is in the range of 20−23° and in accord with previous solid-state NMR measurements. However, AGG, unlike APG or GGV, has a distorted peptide plane, and δ_{11} lies approximately in the plane of N, C$^{\alpha}$, and H rather than in the peptide plane defined by heavy atoms. Accurate orientations of δ_{22} and δ_{33} were determined, and the usual assumption that δ_{22} is along the peptide normal was found only in APG which has a highly nonaxial tensor. More generally, δ_{22} and δ_{33} are rotated about the δ_{11} axis (36° in GGV). These results are compared with DFT calculations to gain a structural understanding of the effects of intermolecular interactions on shielding tensor principal components and orientations. Trimeric clusters containing H-bonded neighbors predict the orientations of the principal components within 2−3°, but calculated principal components are less quantitative. Possible reasons for this disagreement are explored.

Introduction

A central feature of most NMR experiments is chemical shielding. While isotropic shifts are most familiar, there is increasing emphasis on methods for structural and dynamical characterization of proteins that utilize shielding anisotropy, i.e., the full shielding tensor resulting from the nonspherical distribution of electron density surrounding a probe nucleus. Examples in solution NMR are studies of protein dynamics by ^{15}N relaxation and the use of residual anisotropic shielding for constraints in structure determination of weakly aligned proteins. In solids, structural features such as relative peptide plane orientations of proteins embedded in lipid bilayers can be determined if the ^{15}N tensor in each peptide plane is known. Despite the importance of amide ^{15}N tensors, the factors governing their magnitude and orientations are not well understood. Increasingly, principal components (eigenvalues) and orientations (eigenvectors) of shielding tensors are obtained by quantum chemical computation. Embedded in these computations are assumptions about the level of theory, basis sets, intermolecular interactions, hydrogen positions, etc. Thus, for testing theoretical procedures and interpreting a variety of experiments, accurate experimental determination of shielding tensors that systematically sample relevant structures are essential.

Various solution[1−3] and solid-state NMR methods have been used for determining tensor magnitudes and orientations.[4−7] Relaxation-based, solution NMR studies[1−3] have made the approximation that the ^{15}N tensors are axially symmetric, and in one case, site-specific tensors were reported for a small protein, ubiquitin. In a recent study of weakly oriented ubiquitin,[2] the results based on residual shielding indicated that, on average, amide ^{15}N shielding tensors for β-sheet amides deviate more from axial symmetry than helical residues.

Compared to solution methods, shielding anisotropy is more directly observed in solid-state NMR experiments via spectral frequencies, albeit at the expense of the complexity of the system that can be examined. Tensor principal components can be determined in unoriented samples, and to determine tensor orientation, the chemical shift frequencies must be referenced to a local frame, such as a dipole−dipole vector in an unoriented sample or to the crystallographic frame in an indexed single crystal with a known X-ray structure. In general, powder methods for tensor orientations utilizing a single dipole coupling do not uniquely determine the tensor orientation in the molecular frame[5] since the observed spectrum is invariant to an arbitrary rotation about the dipole−dipole vector. Moreover, in one case, where amide shielding tensors were oriented via $^{15}N-^{1}H$ and $^{15}N-^{13}C$ couplings,[8] the inherent symmetries of the dipole couplings yielded two possible orientations. Generally, these ambiguities are absent in single-crystal studies.

The only reported single-crystal study[7] for a peptide nitrogen was for Gly-Gly·HCl. The most downfield component, δ_{11}, lies

† Current address: National High Magnetic Field Lab, Tallahassee, FL.

(1) Boyd, J. *J. Am. Chem. Soc.* **1998**, *120*, 9692.
(2) Cornilescu, G.; Bax, A. *J. Am. Chem. Soc.* **2000**, *122*, 10143.
(3) Fushman, D.; Tjandra, N.; Cowburn, D. *J. Am. Chem. Soc.* **1998**, *120*, 10947.
(4) Munowitz, M.; Aue, W. P.; Griffin, R. G. *J. Chem. Phys.* **1982**, *77*, 1686.
(5) Oas, T. G.; Hartzell, C. J.; Dahlquist, F. W.; Drobny, G. P. *J. Am Chem. Soc.* **1987**, *109*, 5962.
(6) Hartzell, C. J.; Whitfield, M.; Oas, T. G.; Drobny, G. P. *J. Am.Chem. Soc.* **1987**, *109*, 5966.
(7) Harbison, G. S.; Jelinski, L. W.; Stark, R. E.; Torchia, D. A.; Herzfeld, J.; Griffin, R. G. *J. Magn. Reson.* **1984**, *60*, 79.
(8) Chekmenev, E. Y.; Zhang, Q.; Waddell, K. W.; Mashuta, M. S.; Wittebort, R. J. *J. Am. Chem. Soc.* **2004**, *126*, 379.

10.1021/ja044204h CCC: $30.25

in the peptide plane at an angle of 21.3° relative to the N−H bond. Because the tensor is nearly axially symmetric, orienting δ_{22} (and δ_{33}) in the plane perpendicular to δ_{11} was not possible. Single crystal results reported here are for two glycyl amide nitrogens, in the centers of GGV or AGG, and the imide nitrogen in APG. In all three cases, the tensor components are sufficiently different that the complete tensor orientation is determined. The angle β, between δ_{11} and the N−H or N−C$^{\delta}$ (pro) bonds, is 20° or 23°. These are in excellent agreement with β values determined from $^{15}N-^{1}H$ dipolar couplings in powder spectra for these[8] as well as other peptides[9] but are somewhat larger than the 16−19° range obtained from solution NMR relaxation[1,3] and residual shielding[2] measurements in proteins. We find that in AGG, where the N−H bond is out of the peptide plane, δ_{11} is similarly out of the plane. Finally, the usual assumption that δ_{22} is along the peptide plane normal is found to be approximately correct only in APG where the tensor is highly nonaxial. More generally, δ_{22} (and δ_{33}) can be rotated about the δ_{11} axis by a substantial amount, 36° in GGV. With the aim of quantitatively understanding the experimentally determined tensors, they are compared with DFT calculations of isolated molecules and small clusters constructed from the X-ray structure. The cluster calculations, which contain only directly H-bonded neighbors, predict the orientations of the principal components within 2−3° but are less quantitative in predicting tensor principal component magnitudes.

Experimental Methods

Peptide Synthesis and Crystallization. ^{15}N-labeled amino acids were purchased from Cambridge Isotope Laboratories (Andover, MA) and converted into boc-protected amino acids by reaction with *tert*-butyloxycarbonyl anhydride in *tert*-butyl alcohol under basic conditions. Ala-[^{15}N]Pro-Gly (APG), Gly-[^{15}N]Gly-Val (GGV), and Ala-[^{15}N]Gly-Gly (AGG) were prepared by standard solid-phase synthesis with boc-protected amino acids as previously described.[8]

Crystals of labeled APG, GGV, and AGG were grown by vapor diffusion by equilibrating saturated aqueous solutions with ethylene glycol inside silanized glass chambers. Single crystals weighing 0.1−1 mg with clearly defined faces were harvested for NMR. Crystallographic symmetry was exploited in each case to unambiguously confirm the location of axes as determined from X-ray experiments.

The crystal structure of APG·H_2O (CSD code FUDGIU)[10] has been previously reported. APG crystallizes in the orthorhombic space group, $P2_12_12_1$, with four molecules in the unit cell. In this space group, rotations about the *a*, *b*, or *c* axes should therefore result in the observation of two magnetically inequivalent nuclei.

GGV·$2H_2O$ (CUWRUH)[11] and AGG·H_2O (CALXES20)[12] both crystallize in the monoclinic space group, $P2_1$, with two molecules in the unit cell and $\gamma = 93.85$ or 102.14, respectively. Therefore only one magnetically inequivalent nucleus should be observed when either GGV or AGG is rotated about the *b*-axis. Additional structural details, including atomic coordinates, anisotropic displacement parameters as well as complete lists of bond lengths, angles, and torsion angles, can be obtained at www.ccdc.cam.ac.uk/conts/retrieving.html.

NMR Spectroscopy. ^{15}N NMR spectra were acquired at 11.7 T (^{15}N frequency equal to 50.2 MHz) on a home-built spectrometer with a double resonance (^{1}H,^{15}N) probe based on a previously described design.[13] ^{15}N transients were acquired with 2 s recycle delays using 2−3 ms Hartman-Hahn contacts ($\gamma B_1^N/2\pi = \gamma B_1^H/2\pi = 40$ kHz) followed by ^{1}H CW decoupling (50 kHz). Experimental line widths ranged from 100 to 200 Hz, and spectra with S/N ratios of ≥20:1 were accumulated in less than 1k transients. Rotations were generated by turning a matched worm gear assembly with a dial indicator located outside the magnet. Orientation dependence of shielding tensors about three orthogonal axes {*i*,*j*,*k*} were sampled in 5° increments over a range of 200°. Chemical shielding tensor components in the {*i*,*j*,*k*} frame were extracted from *i*-axis rotation curves via linear least-squares fitting to the function:

$$\delta^{(i)} = \frac{1}{2}(\delta_{jj} + \delta_{kk}) + \frac{1}{2}(\delta_{jj} - \delta_{kk})\cos(2\phi) - (\delta_{jk})\sin(2\phi) \quad (1)$$

with cyclic permutations of the indices. The eigenvalues and corresponding eigenvectors of this tensor are, respectively, the principal shielding components and their vector orientations in the {*i*,*j*,*k*} frame. X-ray crystallography was used to determine the transformation from the {*i*,*j*,*k*} frame to the crystallographic {*a* or *a**,*b*,*c* or *c**} frame. Eigenvalues (principal components) were referenced externally to solid $^{15}NH_4Cl$ and then indirectly to liquid NH_3 using δ_{iso} ($^{15}NH_4Cl$, solid) = 39.1 ppm.[14]

Theoretical Calculations. ^{15}N shielding tensors were calculated with density functional theory (DFT) and the gauge including atomic orbitals (GIAO)[15−18] approach as implemented in Gaussian-98.[19] Clusters of APG, GGV, and AGG were constructed as described below using the published coordinates.[10−12] Hydrogen coordinates were optimized at B3LYP/6-31g(d,p), depending on available resources. For comparison with experiment, calculated shielding components, σ_{ij}, were converted to chemical shifts, δ_{ij}, using the conversion, $\delta_{ij} = 244.6 - \sigma_{ij}$, suggested by the work of Jameson and co-workers.[20,21]

Results and Discussion

Single-Crystal NMR. Spectrum frequencies obtained by rotating a single crystal of APG about the crystallographic {*a*, *b*, *c*} axes are shown in Figure 1. Rotation curves are consistent with expectations based on space group symmetry in APG. Although there are four crystallographically inequivalent nuclei in the unit cell, only two unique projections onto the magnetic field are expected when rotation is coincident with a crystal axis. This favorable attribute of the APG crystal symmetry was used to minimize two error sources in single-crystal NMR: crystal misalignment and inaccurate (nonorthogonal) reorientations. Fine adjustments to the crystal's orientation on the goniometer axle were made prior to data collection to ensure

(9) Lee, D. K.; Wittebort, R. J.; Ramamoorthy, A. *J. Am. Chem. Soc.* **1998**, *120*, 8868.
(10) Wu, S.; Declerq, P.; Tinant, B.; Van Meerssche, M. *Bull. Soc. Chim. Belg.* **1987**, *96*, 515.
(11) Lalitha, V.; Subramanian, E.; Bordner, J. *Int. J. Pept. Protein Res.* **1984**, *27*, 223.
(12) Subramanian, E.; Lalitha, V. *Biopolymers* **1983**, *22*, 833.
(13) Zhang, Q. W.; Zhang, H.; Lakshmi, K. V.; Lee, D. K.; Bradley, C. H.; Wittebort, R. J. *J. Magn. Reson.* **1998**, *132*, 167.
(14) Hayashi, S.; Hayamizu, K. *Bull. Chem. Soc. Jpn.* **1991**, *64*, 688.
(15) Ditchfield, R. *J. Mol. Phys.* **1974**, *27*, 789.
(16) Wolinski, K.; Hinton, J. F.; Pulay, P. *J. Am. Chem. Soc.* **1990**, *112*, 8251.
(17) Rauhut, G.; Puyear, S.; Wolinski, K.; Pulay, P. *J. Phys. Chem.* **1996**, *100*, 6310.
(18) London, F. *Phys. Radium* **1937**, *8*, 397.
(19) Frisch, M. J.; Trucks, G. W.; Schlegel, H. B.; Scuseria, G. E.; Robb, M. A.; Cheeseman, J. R.; Zakrzewski, V. G.; Montgomery, J. A., Jr.; Stratmann, R. E.; Burant, J. C.; Dapprich, S.; Millam, J. M.; Daniels, A. D.; Kudin, K. N.; Strain, M. C.; Farkas, O.; Tomasi, J.; Barone, V.; Cossi, M.; Cammi, R.; Mennucci, B.; Pomelli, C.; Adamo, C.; Clifford, S.; Ochterski, J.; Petersson, G. A.; Ayala, P. Y.; Cui, Q.; Morokuma, K.; Malick, D. K.; Rabuck, A. D.; Raghavachari, K.; Foresman, J. B.; Cioslowski, J.; Ortiz, J. V.; Baboul, A. G.; Stefanov, B. B.; Liu, G.; Liashenko, A.; Piskorz, P.; Komaromi, I.; Gomperts, R.; Martin, R. L.; Fox, D. J.; Keith, T.; Al-Laham, M. A.; Peng, C. Y.; Nanayakkara, A.; Gonzalez, C.; Challacombe, M.; Gill, P. M. W.; Johnson, B.; Chen, W.; Wong, M. W.; Andres, J. L.; Gonzalez, C.; Head-Gordon, M.; Replogle, E. S.; Pople, J. A. *Gaussian98*, Revision A.7 ed.; Gaussian, Inc.: Pittsburgh, PA, 1998.
(20) Jameson, C. J.; Jameson, A. K.; Cohen, S. M.; Parker, H.; Opposunggu, D.; Burrell, P. M.; Wille, W. *J. Chem. Phys.* **1981**, *74*, 1608.
(21) Jameson, C. J.; de Dios, A. C.; Jameson, A. K. *J. Chem. Phys.* **1991**, *95*, 1069.

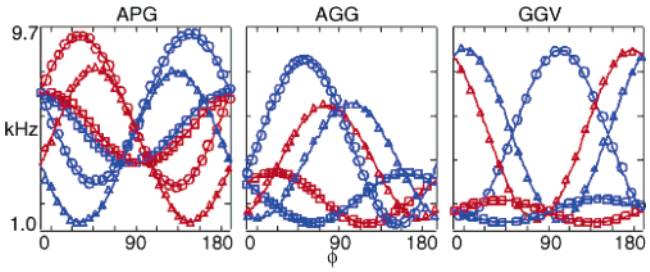

Figure 1. ^{15}N NMR frequencies as a function of crystal orientation for APG, AGG, and GGV. Frequencies for symmetry related pairs (red and blue) shown for crystal rotations about the *a* (squares), *b* (circles), and *c* or *c** (triangles) axes.

Table 1. APG, GGV, and AGG ^{15}N Shielding Tensor Principal Components (ppm relative to NH_3(l))

	δ_{11}	δ_{22}	δ_{33}	δ_{iso}	δ_{span}	δ_{dev}
			APG			
SC	231(2)	127(2)	38(2)	132(2)	194	89
static	232(5)	126(5)	37(5)	132(5)	195	89
MAS	232(3)	124(3)	41(3)	132.4(0.5)	190	82
DFT	234	147	41	141	193	106
			AGG			
SC	207(2)	59(2)	48(2)	105(2)	159	11
MAS	210(3)	56(3)	49(3)	104.8(0.5)	162	7
DFT	216	71	53	113	163	18
			GGV			
SC	218(2)	63(2)	53(2)	111(2)	164	10
MAS	220(3)	63(3)	56(3)	112.8(0.5)	164	7
static	220(5)	60(5)	50(5)	110	170	10
DFT	227	74	64	122	163	10

proper alignment and the observation of two magnetically inequivalent nuclei. Fitting the curves in Figure 1 to eq 1 results in the double- and four-fold determination of off-diagonal and diagonal shielding tensor components, respectively. These components were averaged and the plus/minus combinations of off-diagonal elements were used to construct eight shielding tensors consistent with experimental data. Two unique sets of eigenvalues, each with four sets of symmetry-related eigenvectors, result from diagonalizing these eight tensors.

The correct set of eigenvalues was chosen by comparison with principal components determined from stationary and slow-spinning MAS powder spectra, Table 1. Principal components obtained from single crystal, MAS, and static experiments are in excellent agreement, indicating that three accurate, orthogonal crystal rotations were performed for all samples. Assignment of the four sets of eigenvectors to each of the symmetry-related molecules in the unit cell was unambiguously made by discarding assignments in which the angle between δ_{11} and the pro N−C$^{\delta}$ bond was not in the range of 15°−25°.

Single-crystal rotations for AGG and GGV, Figure 1, are similar and distinct from APG. As required by their crystallographic symmetries, the two molecules of each unit cell are magnetically equivalent when the rotation axis is collinear with the crystal *b*-axis, while rotations about axes orthogonal to the *b*-axis give a pair of curves which cross at 0° and 90°. Data analysis is similar to that in APG, but only two pairs of symmetry-related tensors are obtained in both AGG and GGV. As before, the spurious pairs of eigenvalues were eliminated by comparing crystal and powder sample (MAS or stationary) eigenvalues, and assignment to specific molecules in the unit cell was based on the published value of β (20°) in GGV[8] and the expectation of a similar value for AGG.

Table 2. Molecular Orientations of Central Residue ^{15}N Shielding Tensors in APG, AGG, and GGV[a]

	δ_{11}	δ_{22}	δ_{33}	x	y	z
			APG			
a	0.359	−0.643	−0.667	−0.741	−0.631	0.230
b	0.660	−0.337	0.671	0.483	−0.263	0.835
c	0.660	0.688	−0.303	−0.466	0.730	0.499
			AGG			
a	−0.534	0.252	−0.807	−0.610	0.263	−0.748
b	0.187	−0.896	−0.403	−0.602	−0.768	0.220
*c**	0.825	0.366	−0.431	−0.516	0.584	0.627
			GGV			
a	−0.962	−0.271	0.044	0.0660	−0.262	0.963
b	0.196	−0.564	0.802	0.263	−0.926	−0.270
*c**	−0.193	0.780	0.596	0.963	0.271	0.008

[a] Eigenvectors are labeled by their corresponding principal component, and reference vectors are defined as follows: *x* is along N−C′, *y* is normal to the plane containing N, C′, C$^{\alpha}$, and *z* is orthogonal to *x* and *y*.

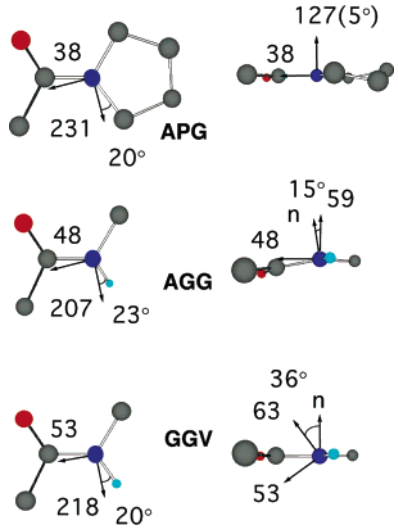

Figure 2. Molecular orientations of principal shielding axes. On the left, peptide planes are in the plane of the figure, and on the right, views are down the δ_{11} axes with the peptide planes approximately orthogonal to the plane of the figure. **n** is the peptide normal defined by heavy atoms (see text), and the eigenvectors are labeled by their corresponding principal components (ppm).

The experimentally determined eigenvectors for the central residue nitrogens in the three peptides are listed in Table 2. Also listed are reference frames based on the peptide planes in the orthogonal crystallographic frames. These orientations are depicted in Figure 2. In the central peptide linkage of APG, δ_{11} is 23° from the N−C$^{\delta}$ bond and 5° below the peptide plane. The orientations of δ_{22}, 4° from the peptide plane normal, and δ_{33}, approximately in the peptide plane, are both accurately determined since the tensor is highly nonaxial. Comparing theory with experiment, Table 3, shows that calculated tensor orientations are within 3° and are not strongly affected by the size of the APG cluster.

In AGG, δ_{11} is 11° out of the peptide plane defined by accurate heavy atom positions (N(gly-2), C$^{\alpha}$(gly-2), and C′(ala-1)), and δ_{22} is rotated by 15° from the plane normal. However, if the plane is defined to contain the amide proton rather than C′(ala-1), δ_{11} does lie in the plane, and δ_{22} is closer to the normal. In this structure, the N−H bond vector deviates 12° from the plane and points toward a hydrogen-bonded oxygen on an adjacent molecule in the crystal lattice. We note that DFT

Table 3. Comparison of Experimental and Theoretical Principal Shielding Orientations[a]

molecule		$\beta°$	$\gamma°$	$\phi°$
APG	single	20	2	3
	trimer	23	2	3
	exp.	23(3)	5(3)	5(3)
AGG	single	18	9	16
	trimer	23	8	12
	exp.	20(3)	11(3)	15(3)
GGV	single	13	0	12
	trimer	17	0	32
	exp.	23(3)	1(3)	36(3)

[a] β is the angle between δ_{11} and the N−H bond, γ is between δ_{11} and the peptide plane, and ϕ is between δ_{22} and the peptide plane normal. The peptide frame is that defined in Table 2 and is based on heavy atom positions.

optimization of the amide hydrogen coordinate results in a small change of the N−H bond direction (1.5° closer to the plane) compared to the X-ray coordinates, indicating that the out-of-plane orientation likely results from hydrogen-bonding interactions. Importantly, the DFT calculated principal axis orientations are within 3° of their experimental counterparts.

The orientation in GGV is distinct. In accord with expectations, the most deshielded axis is 1° out of the peptide plane and 23° from the N−H bond, but the δ_{22} and δ_{33} axes are substantially rotated about δ_{11} such that δ_{22} is off of the peptide plane normal by 36°. This possibility was suggested by experiments on unoriented samples and by calculations,[22,23] but this is the first single-crystal study confirming this. DFT calculations on the cluster, more fully described in the next section, predict the observed orientation.

Calculations. To explore the underlying structural basis for the experimental results, we have used quantum chemical computations.[23] Important features of the calculations include molecular geometry**,** the level of theory, basis set, cluster construction, and the conversion from calculated shieldings, σ, to experimental shifts, δ, referenced to liquid ammonia. For the latter, we have used $\delta = 244.6 - \sigma$, which depends on a calculated isotropic shift of NH_4(g), 264.0 ppm, and the experimentally observed difference, 19.4 ppm, between NH_3(g) and the reference, NH_3(l).[20,21] To specify tensor components, we use the isotropic shift and two parameters that are independent of this conversion; the tensor span, $\delta_{span} = \delta_{11} - \delta_{33}$, and deviation from axial symmetry, $\delta_{dev} = \delta_{22} - \delta_{33}$. Initially, we found that DFT calculations were in better agreement with experiment than Hartree−Fock calculations, and these are not discussed further. Otherwise, methods used to obtain the tensors in Tables 1 and 3 were initially assessed with APG models because of the absence of an N−H bond at the prolyl nitrogen. This ensures accurate X-ray coordinates of atoms adjacent to the target nitrogen that potentially have a substantial effect on shielding calculations. For example, DFT tensor components in benzamide showed differences of 2−10 ppm between calculations using hydrogen positions obtained from neutron diffraction or by quantum chemical optimization.[24]

To examine basis set convergence, DFT calculations on monomers with increasing size of the basis set are shown in Figure 3. Included are calculations using the correlation consistent, split valence basis sets that are known to extrapolate smoothly to a complete basis with increasing number of orbital exponents.[25] We find that all calculated shielding parameters converge to within ~2 ppm of extrapolated values at the aug-cc-pv5z level or within 2−3 ppm with aug-cc-pvqz. However, these large basis sets are prohibitive for the molecular clusters of interest here, and the smaller Pople set, 6-311++g(d,p), with 60% of the basis functions of aug-cc-pvtz performs almost as well as aug-cc-pvqz. Compared to converged values, individual tensor components and δ_{iso} are shifted upfield by 5−7 ppm and δ_{span} and δ_{dev} are underestimated by 3−4 ppm. Alternative functionals, B3P86 or B3PW91, showed an additional small upfield isotropic shift but were otherwise equivalent to B3LYP.

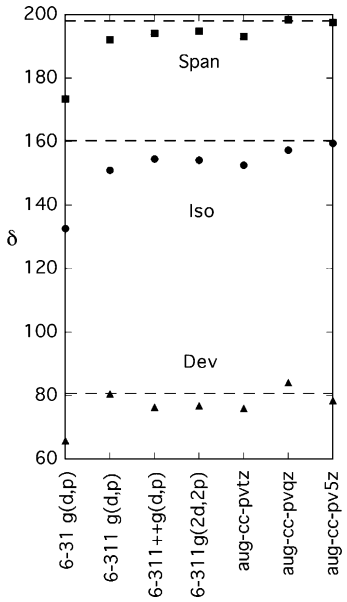

Figure 3. Basis set dependence of δ_{span}, δ_{iso}, and δ_{dev} for DFT calculations on a single molecule of APG in its crystallographically determined conformation. Dotted lines are for values extrapolated to infinite basis set using results from the Dunning correlation consistent set, aug-cc-pvdz (not shown) to aug-cc-pv5z.

Variations of shielding parameters with cluster size are shown and compared with the experimental data (dotted lines) in Figure 4. The monomer calculation reasonably predicts the experimental tensor span, substantially overestimates the isotropic shift (23 ppm) and underestimates the deviation from axial symmetry (13 ppm). These errors are qualitatively inconsistent with those expected from basis set truncation alone. Previously it has been demonstrated[26] that H-bonding substantially shifts δ_{iso} and δ_{22} for histidyl nitrogens downfield. Furthermore, Grant and Strohmeier have shown that an electrostatic model[27] for both H-bonds and partial atomic charges affects ^{15}N isotropic shifts more substantially, 10−30 ppm, relative to the isolated molecule.

To account for intermolecular interactions, we use dimer and trimer clusters.[28] In the APG dimer, Figure 5, the molecule in the crystal lattice which forms the gly → ala indirect H-bond ($r_{N...O}$ = 3.157 Å) at the target amide is added. The two molecules with 3_1-helical conformations ($\phi/\psi = -67°/-158°$)

(22) Brender, J. R.; Taylor, D. M.; Ramamoorthy, A. *J. Am Chem. Soc.* **2001**, *123*, 914.
(23) Walling, A. E.; Pargas, R. E.; de Dios, A. C. *J. Phys. Chem. A* **1997**, *101*, 7299.
(24) Facelli, J. C.; Pugmire, R. J.; Grant, D. M. *J. Am. Chem. Soc.* **1996**, *118*, 5488.
(25) Dunning, T. H. *J. Chem. Phys.* **1989**, *90*, 1007.
(26) Wei, Y. F.; de Dios, A. C.; McDermott, A. E. *J. Am. Chem. Soc.* **1999**, *121*, 10389.
(27) Strohmeier, M.; Grant, D. M. *J. Am. Chem. Soc.* **2004**, *126*, 966.
(28) Orendt, A. M.; Facelli, J. C.; Grant, D. M. *Chem. Phys. Lett.* **1999**, *302*, 499.

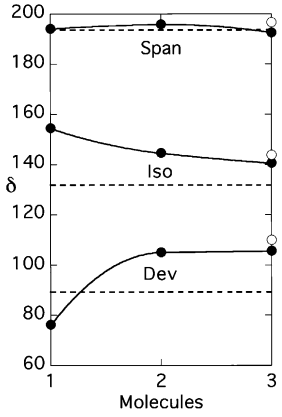

Figure 4. Variation of DFT 6-311++g(d,p) (●) and DFT aug-cc-pvqz (○) shielding parameters with cluster size in APG. Curves are to guide the eye, and dotted lines are experimental values.

are arranged side-by-side and antiparallel so that they are salt-bridged at the charged N- and C-termini. In the trimer, a molecule H-bonded to the target molecule's terminal gly amide is added, resulting in a sheetlike cluster. Note that the trimer lacks the local charge neutralization in the dimer, but overall, the cluster is neutral. Forming the dimer results in δ_{11} and δ_{33} moving upfield together, while δ_{22} moves downfield. Compared to experiment, δ_{iso} is under corrected, δ_{dev} is over corrected, and δ_{span} is in good agreement with experiment independent of cluster size. A neutral monomer calculation, wherein a proton was moved from the N-terminus to the C-terminus, resulted in changes qualitatively similar to that in the clusters, indicating that electrostatics apart from H-bonding are important.

The crystal structures of AGG and APG are similar. Consequently, we have also used a sheetlike structure containing three antiparallel tripeptides for the AGG cluster ($\phi/\psi = -83°/169°$), Figure 5. However, the absence of an imino acid results in a different H-bonding arrangement. The target amide group has a direct H-bond ($r_{N\cdots O} = 2.93$ Å) to the central gly C═O of the peptide on one side of the sheet and an indirect link ($r_{N\cdots O} = 3.00$ Å) to the terminal gly N−H of the other flanking peptide. Also, unlike APG, the charged termini of the target peptide are proximal (salt-bridged) only to the termini of the indirectly H-bonded molecule. The GGV cluster retains the α−helical features ($\phi/\psi = -77°/-22°$) of the GGV dihydrate X-ray structure[11] in which each tripeptide and a water molecule form one turn of the helix, Figure 5. The cluster contains three GGV molecules and their bridging waters, thus placing the target glycyl amide in the middle of a three-turn helix. The waters, which are strongly held,[29] also bridge the N- and C-termini within a peptide unit.

Experimental agreement of calculated shielding parameters in the GGV and AGG clusters is similar to that in APG with the improvement that δ_{dev} values are either less overestimated (7 ppm in AGG) or equivalent to experiment (GGV). Removal of the waters in the GGV cluster substantially reduces the agreement with experiment. Like APG, δ_{span} values are again in excellent agreement with experiment, and δ_{iso} is deshielded by 8 or 9 ppm relative to experiment, i.e., tensor components are consistently deshielded by 5−13 ppm relative to experiment.

It has been noted in the literature that principal axis orientations are less sensitive to basis set than principal components.[22] This is not unexpected since, for any matrix, such as a shielding tensor, small errors in the matrix elements affect eigenvalues in first order, whereas eigenvectors are only affected in second and higher order. It is thus of interest to compare the experimental tensor orientations with calculations, Table 3, to discern what is required to model the unexpected orientations in GGV and AGG.

The extent that δ_{11} is rotated away from the N−H bond, β, increases from single molecule to trimer, with the latter in better agreement with experiment. This effect is smaller in APG, which does not have a direct hydrogen bond, and larger in AGG and GGV, indicating that this parameter is affected by H-bonding. Calculated values of γ (how far δ_{11} is out of the peptide plane) are in excellent agreement with experiment and are insensitive to cluster construction. In AGG, the result does depend on the nonplanar peptide conformation discussed above. The single-molecule calculations show that approximate symmetry arguments placing δ_{22} along the peptide plane normal ($\phi = 0$) are incorrect for GGV and AGG, independent of intermolecular effects. Moreover, intermolecular effects on ϕ are large in GGV which is strongly H-bonded ($r_{N\cdots O} = 2.78$ Å) and has a nearly axial tensor ($\delta_{dev} = \delta_{22} - \delta_{33} = 10$ ppm). In contrast, $\phi \sim 0$ and calculated intermolecular effects are absent in APG which lacks a direct H-bond and has a highly nonaxial tensor, $\delta_{dev} = 89$ ppm.

Concluding Remarks

^{15}N principal components and orientations in central residues of APG, GGV, and AGG were measured by single-crystal NMR at 11.7 T. The results are in good agreement with (i) principal components and isotropic shifts measured by slow-spinning MAS[8] and (ii) with the known crystallographic symmetry of the samples examined, thus indicating the accuracy of the single-crystal results reported here. Some aspects of the tensor orientations are as expected; however, only the imide tensor orientation in APG conforms closely to that typically assumed for a peptide nitrogen. The range of angles between the most shielded component, δ_{11}, and the N−H bond is small, 20−23°. These are consistent with data obtained using the ^{15}N−^{1}H dipolar coupling in crystalline powders[8,9] and greater than that estimated by NMR relaxation in proteins.[2] Also, δ_{11} is in the peptide plane within 3° if defined by N, C$^{\alpha}$, and H rather than by N, C$^{\alpha}$, and C′. Defining the plane in these two ways is different in AGG since the central peptide unit is not planar as a result of the H-bonding geometry. The surprising result is that δ_{22} and δ_{33} can be rotated about δ_{11} such that δ_{22} is not along the peptide normal and δ_{33} lies out of the peptide plane. In the three examples studied here, this rotation, ϕ, increases substantially as the difference between these two components, δ_{dev}, decreases. Thus $\phi = 6°$ (APG), 15°(AGG) and, 36° (GGV), respectively, for $\delta_{dev} = 89$ ppm, 11 ppm and, 10 ppm. Since α-helical residues typically have small tensor asymmetry,[2,8] they are likely sites for this unexpected result.

The observed tensor orientations are in good agreement (error ≤ 3°) with DFT cluster calculations. The AGG and GGV orientations are sensitive to intermolecular effects discerned by comparing single molecule with cluster calculations,[22,30] while the highly asymmetric APG tensor is not. Noteworthy in this

(29) Pometun, M. S.; Gundusharma, U. M.; Richardson, J. F.; Wittebort, R. J. *J. Am Chem. Soc.* **2002**, *124*, 2345.
(30) Zhang, Q.; Chekmenev, E. Y.; Wittebort, R. J. *J. Am. Chem. Soc.* **2003**, *125*, 9140.

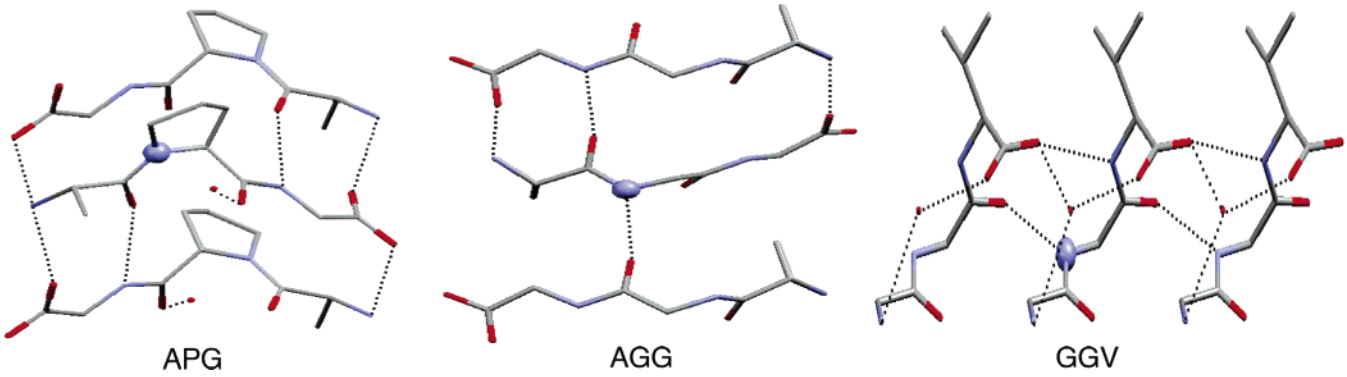

Figure 5. Structures of the APG, AGG, and GGV trimers used in the DFT calculations. The target nitrogen is enlarged, and H-bonds are shown with dotted lines.

regard is the large ϕ rotation in GGV. By systematically stripping away neighboring waters and GGV molecules, it was observed that the directly hydrogen-bonded GGV molecule and the terminal spanning water of the target molecule were essential to reproduce experiment.

Overall agreement between calculated and experimental principal components is less satisfactory. The RMS error for calculated tensor components is 10.6 ppm, and they are systematically deshielded relative to experiment. This trend has been noted previously,[22] and in the three cases reported here, isotropic shifts are too deshielded by 8−9 ppm. Since isotropic shifts at B3LYP/6-311++g(d,p) are 5 ppm upfield of the extrapolated basis set limit, this error is not likely due to incomplete basis sets. In addition, since calculations were tested on APG where the target nitrogen lacks directly bound hydrogens, the impact of uncertainties in X-ray coordinates was minimized. Chestnut[31] suggested that DFT methods systematically overestimate the paramagnetic (deshielding) contribution to the chemical shift, and we note that the standard shielding to shift conversion used here is based on a Hartree−Fock/MP-2 as opposed to a DFT calculation.[21] It is noted that RMS error in principle components is minimized (∼5 ppm) if the shielding reference is moved to 235.6 ppm from 244.6 ppm.

Another potential source of error in our calculations is that the electrostatics and magnetic susceptibilities[32] of non-H-bonded neighboring molecules are not adequately accounted for in the trimer clusters. As noted above, the most successful calculation reported here is for GGV wherein the target is buried in the center of a three-turn helix, while in the less successful APG and AGG calculations, molecules above and below the sheetlike clusters are absent. Previous work indicates that electrostatic interactions out to a distance of 10 Å can affect ^{15}N shielding.[33] Thus, a judicious increase in cluster size will potentially improve the calculation and provide a basis for understanding the magnetic shielding of a probe nucleus embedded in a protein in terms of local interactions. Insofar as our calculations are already large (∼1500 basis functions), more extensive use of the locally dense method[31] (full basis sets on atoms in the neighborhood of the probe nucleus rather than the entire molecule) would make the calculation feasible.

Acknowledgment. We thank Dr. Mark Mashuta and Dr. John Richardson for indexing APG and GGV and Dr. Sean Parkin for indexing AGG. We thank the University of Kentucky for HP Superdome computing allocation.

Supporting Information Available: Gaussian input files for trimer clusters of APG, AGG, and GGV. This material is available free of charge via the Internet at http://pubs.acs.org.

JA044204H

(31) Chesnut, D. B. *Chem. Phys. Lett.* **2003**, *380*, 251.

(32) Sitkoff, D.; Case, D. A. *Prog. Nucl. Magn. Reson. Spectrosc.* **1998**, *32*, 165.

(33) Scheurer, C.; Skrynnikov, N. R.; Lienin, S. F.; Straus, S. K.; Bruschweiler, R.; Ernst, R. R. *J. Am. Chem. Soc.* **1999**, *121*, 4242.